Chemical Physics 85 (1984) 473–479
North-Holland, Amsterdam

SATURABLE ABSORPTION OF DYES EXCITED TO THE LONG-WAVELENGTH REGION OF THE S_0–S_1 ABSORPTION BAND

W. BLAU, W. DANKESREITER and A. PENZKOFER

Naturwissenschaftliche Fakultät II – Physik, Universität Regensburg, 8400 Regensburg, FRG

Received 12 September 1983

Organic dyes are excited with intense picosecond ruby laser pulses to the long-wavelength wing of the S_0–S_1 transition beyond the fluorescence emission peak. A model is presented where only a fraction of the molecules interacts with laser light and the excitation terminates in the S_1 equilibrium level. Bleaching is readily observed but laser action and amplified spontaneous emission are reduced.

1. Introduction

The dynamics of S_1–S_0 relaxation of dye solutions is determined by the solute, the solvent, and the excitation source. The frequency of excitation influences the relaxation mechanisms: Promotion of molecules to higher singlet states $S_n (n \geq 2)$ opens decay channels mainly to the S_1 state, to the S_0 state, to triplet states and to molecular decomposition [1,2]. For molecules tending to form excited-state conformers the S_1–S_0 decay mechanism depends on the excess energy of the excitation compared to the $S_1(v' = 0)$–$S_0(v'' = 0)$ (zero vibration) transition energy. The excess energy facilitates excited-state isomer formation and opens new decay channels [3–6]. The pump light intensity plays a decisive role in S_1–S_0 relaxation when intense picosecond pulses are used for S_1 state population: amplified spontaneous emission enhances the depopulation of the S_1 state [7,8], excited-state absorption promotes molecules to higher-lying states [9,10] and initiates new decay channels.

The saturable absorption of dyes excited with picosecond laser pulses of frequency ν_L less than the frequency of optimum fluorescence emission $\nu_{F,m}$ is studied in this paper. A realistic model for the absorption and relaxation processes is presented. In contrast to short-wavelength excitation ($\nu_L \gtrsim \nu_{A,m}$, $\nu_{A,m}$ frequency of maximum S_0–S_1 absorption), here the excitation terminates in the temporal equilibrium position of the S_1 state from where the fluorescence emission originates. Only thermally excited molecules or molecules in the long-wavelength tail of the inhomogeneous S_0–S_1 transition frequency distribution can interact with the pump laser. As a consequence the bleaching of dyes is readily observed (only a fraction of molecules absorbs at the long wavelength side) while amplified spontaneous emission and laser action is reduced (re-absorption of fluorescence emission with $\nu > \nu_L$ due to ground-state population). The effects of spectral cross-relaxation in the S_0 band on the absorption dynamics will be discussed.

Experiments are performed on some organic dyes with a passively mode-locked ruby laser. The experimental results confirm the theoretical considerations. Some aspects of pulse propagation in fluorescing dye media have been reported previously [11–16]. Especially dyes with slow solute–solvent relaxation have been studied in refs. [11–15].

2. Theory

The absorption spectrum of dye solutions is rather complex. The S_0 ground-state levels are thermally populated, the S_0–S_1 frequency spacing

0301-0104/84/$03.00

is inhomogeneously broadened due to irregular actions of the solvent, and a manifold of transitions between S_0 and S_1 rovibrational levels are possible at a fixed laser frequency ν_L. Additionally each transition is homogeneously broadened by phase changes and finite population lifetimes. Reduction of this multi-transition problem to a four-level system was achieved in ref. [17] for $\nu_L \gtrsim \nu_{A,m}$. Necessary conditions for the reduction are that either the spectral cross-relaxation is fast compared to the pump pulse duration or approximately all molecules take part in the absorption with nearly equal absorption coefficients. The four-level description may be applied approximately to the frequency region $\nu_{A,m} > \nu_L > \nu_{F,m}$. It breaks down for $\nu_L \leqslant \nu_{F,m}$ since for this case the population of the lower level 1 (fig. 3 of ref. [17]) is only a fraction of the total S_0 state population and the excitation terminates most probably in the minimum of the S_1 potential curve (levels 2 and 3 of fig. 3 in ref. [17] coincide).

The situation of long-wavelength excitation $\nu_L \leqslant \nu_{F,m}$ is displayed in fig. 1. In part (a) a single-minimum potential distribution is depicted which describes our investigated dyes with normal Stokes shifted fluorescence spectra. The presented theory applies also to the saturable absorption of dyes which form excited-state isomers if the time constant of isomer formation is long compared to the pump pulse duration. In this case the local S_1 potential minimum populated within the pump pulse duration would be relevant.

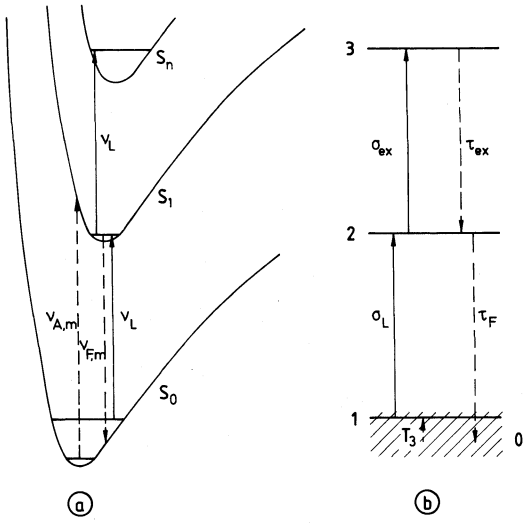

Fig. 1. (a) Potential-energy diagram. (b) Level system relevant for long-wavelength excitation.

In fig. 1b a realistic level system is extracted from the potential curves of fig. 1a. Level 1 indicates the states of molecules (thermally excited and/or in the long-wavelength wing of an inhomogeneous distribution) that take part in the S_0–S_1 transition by laser light absorption. Level 2 represents the low-lying states around the S_1 potential minimum. Level 3 comprises the states in an S_n band reached by S_1–S_n excited-state absorption. Level 0 represents the whole S_0 band including level 1. The extension of population in level 0 (S_0 band) is indicated by the dashed region. Inclusion of level 1 in level 0 simplifies the calculations. The dynamics of this level system is governed by the following system of differential equations ($t' = t - \eta z/c$; t time; z distance; η refractive index; c light velocity in vacuum):

$$\frac{\partial N_1(\theta)}{\partial t'} = -\frac{3I_L}{h\nu_L}\sigma_L \cos^2\theta\,[N_1(\theta) - N_2(\theta)] - \frac{N_1(\theta) - \bar{N}_1}{\tau_{or}} - \frac{N_1(\theta) - \rho_A N_0(\theta)}{T_3}, \quad (1)$$

$$\frac{\partial N_2(\theta)}{\partial t'} = \frac{I_L}{h\nu_L}\{3\sigma_L \cos^2\theta\,[N_1(\theta) - N_2(\theta)] - \sigma_{ex}[N_2(\theta) - N_3(\theta)]\} - \frac{N_2(\theta)}{\tau_F} + \frac{N_3(\theta)}{\tau_{ex}} - \frac{N_2(\theta) - \bar{N}_2}{\tau_{or}}, \quad (2)$$

$$\frac{\partial N_3(\theta)}{\partial t'} = \frac{I_L}{h\nu_L}\sigma_{ex}[N_2(\theta) - N_3(\theta)] - \frac{N_3(\theta)}{\tau_{ex}} - \frac{N_3(\theta) - \bar{N}_3}{\tau_{or}}, \quad (3)$$

$$\frac{\partial N_0(\theta)}{\partial t'} = -\frac{3I_L}{h\nu_L}\sigma_L \cos^2\theta\,[N_1(\theta) - N_2(\theta)] + \frac{N_2(\theta)}{\tau_F} - \frac{N_0(\theta) - \bar{N}_0}{\tau_{or}}, \quad (4)$$

$$\frac{\partial I_L}{\partial z} = -I_L\left(3\sigma_L\int_0^{\pi/2}[N_1(\theta) - N_2(\theta)] \times \cos^2\theta \sin\theta\,d\theta + \sigma_{ex}\bar{N}_2\right), \quad (5)$$

$$\bar{N}_i = \int_0^{\pi/2} N_i(\theta)\sin\theta \mathrm{d}\theta \quad (i = 0, 1, 2, 3). \tag{6}$$

The initial conditions are

$$N_0(\theta, r, t' = -\infty, z) = N,$$

$$N_1(\theta, r, t' = -\infty, z) = \rho_A N = \alpha(\nu_L)/\sigma_L,$$

$$N_2(\theta, r, t' = -\infty, z) = N_3(\theta, r, t' = -\infty, z) = 0,$$

and

$$I_L(r, t', z = 0) = I_{0L} g(r) f(t').$$

N is the total number density of dye molecules (molecules/cm^3). $\rho_A = \alpha(\nu_L)/(\sigma_L N)$ is the fraction of molecules that interacts with the laser of frequency ν_L. $\alpha(\nu_L)$ (cm^{-1}) is the absorption coefficient at frequency ν_L measured with a spectrophotometer. σ_L(cm^2) is the absorption cross section at ν_L. It is identical to the stimulated emission cross section σ_E at the same frequency ν_L which can be determined from the fluorescence spectrum [18] (see below). $g(r)$ and $f(t')$ are the spatial and temporal pulse profiles, respectively. Gaussian shapes are assumed in the calculations ($g(r) = \exp(-r^2/r_0^2)$; $f(t') = \exp[-(t')^2/t_0^2]$). The energy transmission T_E (ratio of transmitted pulse energy W_T to input energy W_I) of a laser pulse through the sample is obtained by

$$T_E = \frac{\int_0^\infty \int_{-\infty}^{\infty} I_L(r, t', l)\mathrm{d}t'r\mathrm{d}r}{I_{0L}\int_0^\infty g(r)r\mathrm{d}r \int_{-\infty}^{\infty} f(t')\mathrm{d}t'}. \tag{7}$$

The anisotropy of electric dipole interaction is taken into account by $\sigma_L(\theta) = 3\sigma_L \cos^2\theta$. θ is the angle between direction of electric field strength and direction of the S_0–S_1 transition dipole moment. $\bar{N}_i (i = 0, 1, 2, 3)$ denote orientationally averaged population densities. For the excited-state absorption an average cross section σ_{ex} is used. τ_{or} describes the molecular reorientation time. The same τ_{or} values are assumed for all levels. Level 1 is depopulated by laser light and it is refilled by thermalization of the S_0 state distribution (level 0). The time constant of repopulation is the spectral cross-relaxation time T_3.

Excited-state absorption promotes molecules from level 2 to 3. Molecules in level 3 relax fast to lower states, preferably to level 2 as indicated in fig. 1b and eq. (2). The excited-state lifetime τ_{ex} is generally very short [1,2,8]. A value of $\tau_{ex} = 10^{-13}$ s is assumed in our calculations. Absorption from level 3 to higher-lying states is taken into account by setting the last term in eq. (5) equal to $\sigma_{ex}\bar{N}_2$ instead of $\sigma_{ex}(\bar{N}_2 - \bar{N}_3)$ (open system).

From eq. (2) it is readily seen that the population of the S_1 state (level 2) is limited to $N_2(\theta) \leqslant N_1(\theta) \leqslant \rho_A N/(1 + \rho_A)$ due to the balance of absorption and stimulated emission. No refilling of level 1 within the pump duration ($T_3 > \Delta t_L$) would result in $N_2(\theta) \leqslant \rho_A N/2$ while refilling of level 1 ($T_3 < \Delta t_L$) limits the level 2 population to $N_2(\theta) \leqslant \rho_A N/(1 + \rho_A)$. Between level 2 and level 1 no inversion is possible (pulse duration $\Delta t_L \gg$ dephasing time T_2 [19]).

For fluorescence emission with $\nu > \nu_L$ the absorption dominates the stimulated emission since the population density in the S_0 band below level 1 is higher than the population density of level 2 ($N_2 < N_1$). This fact hinders amplified spontaneous emission and laser action in the frequency region $\nu > \nu_L$. Laser action and amplified spontaneous emission are limited to the long-wavelength tail of the fluorescence band $\nu < \nu_L$. For a fixed small-signal dye transmission T_0 at frequency ν_L the amplified spontaneous emission is reduced since the absorption cross section $\sigma_A(\nu_L)$ is larger than the emission cross section $\sigma_E(\nu)$ [17,8]. Amplified spontaneous emission gains importance with increasing pump laser frequency. In the case of $\nu_L \geqslant \nu_{A,m}$, amplified spontaneous emission occurs around the fluorescence emission peak $\nu_{F,m}$. Inversion between S_1 band and terminating fluorescence Franck–Condon state in S_0 band is easily achieved since all molecules take part in the absorption of laser light. For $\nu_L \approx \nu_{A,m}$ the cross sections for absorption and stimulated emission are approximately equal [$\sigma_A(\nu_{A,m}) \approx \sigma_E(\nu_{F,m})$]. For $\nu_L > \nu_{A,m}$ amplified spontaneous emission may become very strong since $\sigma_E(\nu_{F,m}) > \sigma_A(\nu_L)$. For our experimental situation of $\nu_L < \nu_{F,m}$ and $T_0 \geqslant 0.1$ amplified spontaneous emission is negligible [17,8] and not included in eqs. (1)–(6).

Bleaching of the dye (increase of pulse transmission) is readily achieved for $\nu_L < \nu_{F,m}$ as long as the absorption cross section ($\sigma_L = \sigma_E$) remains reasonably large because the number of interacting molecules is reduced [$\rho_A(\nu_L) < 1$]. At a fixed

small-signal transmission T_0 the necessary pulse energy for bleaching should be about the same for $\nu_L \leqslant \nu_{F,m}$ and $\nu_L \approx \nu_{A,m}$ (same σ_L assumed). Bleaching is aggravated for $\nu_L > \nu_{A,m}$ because in this frequency range all molecules of the S_0 state have to be excited to the S_1 state for complete bleaching (σ_L reduces with $\nu_L > \nu_{A,m}$, $\rho_A(\nu_L) \approx 1$)

3. Experimental

The energy transmission of single picosecond ruby laser pulses ($\Delta t_L \approx 25$ ps) through some dyes has been measured. The laser system and the experimental arrangement are the same as in ref. [20].

Delayed probe pulse transmissions were measured with attenuated ruby laser pulses of perpendicular polarization. An appreciable absorption recovery was not observed up to a delay of 300 ps for the dyes with a fluorescence lifetime in the nanosecond range. A remarkably increased relaxation rate due to amplified spontaneous emission is not expected under our experimental conditions (small number density N_2, see eqs. (43) and (44) of ref. [17]).

The absorption spectra of the analyzed dyes were measured at a concentration of 2×10^{-6} mol/ℓ and at the concentration used in the bleaching experiments. The effective absorption cross sections $\bar{\sigma}_A(\nu) = \rho_A(\nu)\sigma_A(\nu) = \alpha(\nu)/N$ were found to be the same for both concentrations indicating that no dimers were present in the used dye solutions [17].

The fluorescence spectra were recorded by measuring the fluorescence signal under an angle of 90° to the propagation direction of the excitation light. Very dilute solutions were used ($\approx 10^{-6}$ mol/ℓ) in order to avoid spectral red-shifts due to re-absorption. An unpolarized 2 mW He–Ne laser was used as excitation source. The fluorescence light was dispersed with a 30 cm spectrograph and registered with a silicon vidicon. The spectra were corrected for the spectral response functions of the spectrograph and the vidicon.

The effective stimulated emission cross section $\bar{\sigma}_E(\nu) = \rho_E(\nu)\sigma_E(\nu)$ is calculated from the S_1 radiative lifetime τ_{rad} and the spectral shape $E(\nu)$ (quantum distribution, $\int E(\nu)\mathrm{d}\nu = 1$, ν in Hz) of the fluorescence signal according to [18]

$$\bar{\sigma}_E(\nu) = c^2 E(\nu)/8\pi\eta^2\nu^2\tau_{rad}. \tag{8}$$

$\rho_E(\nu)$ describes the fraction of molecules interacting with light of frequency ν in the emission process. It is $\rho_E(\nu) \approx 1$ for $\nu \leqslant \nu_{F,m}$. τ_{rad} is calculated by use of the Strickler–Berg formula [21,17]

$$\tau_{rad}^{-1} = \frac{8\pi\eta^2}{c^2} \frac{\int E(\nu)\nu^{-1}\mathrm{d}\nu}{\int E(\nu)\nu^{-4}\mathrm{d}\nu} \int \bar{\sigma}_A(\nu)\nu^{-1}\mathrm{d}\nu. \tag{9}$$

4. Results and discussion

The structural formula of the investigated azine dyes (oxazines I–VI; thiazines VII, VIII) and of

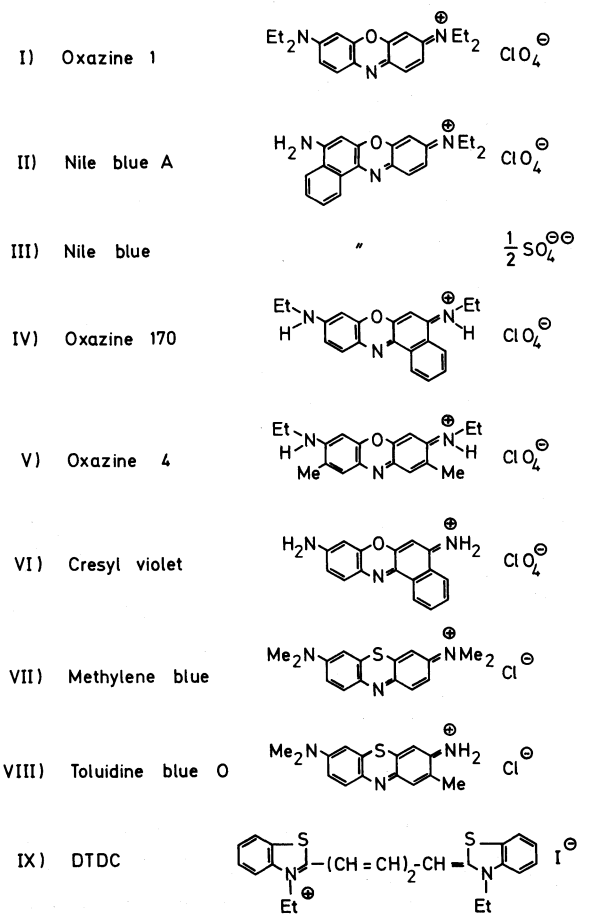

Fig. 2. Structural formulae of investigated dyes.

Table 1
Data of dyes dissolved in ethanol (analytic grade)

Dye	Conc. (mol/ℓ)	$\lambda_{A,m}$ (nm)	$\sigma_{A,m}$ (cm^2)	$\lambda_{E,m}$ (nm)	$\sigma_{E,m}$ (cm^2)	τ_{rad} (ns)	τ_F (ns)	T_0	ρ_A	σ_L (cm^2)	σ_{ex} (cm^2)
methylene blue	1.4×10^{-4}	655	4×10^{-16}	674	2.7×10^{-16}	7.0	0.3 [a]	0.12	5.5×10^{-2}	2.4×10^{-16}	$(3\pm1)\times10^{-17}$
oxazine 1	5.5×10^{-4}	644	4.6×10^{-16}	664	4.2×10^{-16}	5.2	1.02 [b]	0.08	1.5×10^{-2}	2.5×10^{-16}	$(3.5\pm1)\times10^{-17}$
nile blue A	4.8×10^{-4}	635	2.9×10^{-16}	668	3.4×10^{-16}	6.2	1.7 [c]	0.06	1.8×10^{-2}	2.6×10^{-16}	$(8\pm2)\times10^{-17}$
nile blue	6.9×10^{-4}	628	2.6×10^{-16}	662	3.0×10^{-16}	6.8	1.9 [d]	0.12	1.0×10^{-2}	1.7×10^{-16}	$(7\pm1)\times10^{-17}$
toluidine blue 0	7.5×10^{-4}	627	1.5×10^{-16}	658	1.2×10^{-16}	13.7	0.3 [e]	0.10	3.1×10^{-2}	8.6×10^{-17}	$(5\pm1)\times10^{-17}$
oxazine 170	1.1×10^{-3}	624	3.5×10^{-16}	645	4.2×10^{-16}	5.1	3.0 [f]	0.50	2.6×10^{-3}	1.5×10^{-16}	$(6\pm2)\times10^{-17}$
oxazine 4	7.5×10^{-4}	615	3.9×10^{-16}	629	3.5×10^{-16}	5.1	3.2 [g]	0.12	2.1×10^{-2}	1.1×10^{-16}	$(1\pm0.3)\times10^{-16}$
cresyl violet	6.1×10^{-4}	607	2.7×10^{-16}	626	3.2×10^{-16}	5.9	3.51 [b]	0.18	2.8×10^{-2}	8.3×10^{-17}	$(7\pm1)\times10^{-17}$
DTDC	5.1×10^{-5}	655	9.5×10^{-16}	678	9.7×10^{-16}	3.0	1.38 [h]	0.08	5.2×10^{-2}	8.0×10^{-16}	$(9\pm3)\times10^{-17}$

[a] Fluorescence quantum efficiency $q_F = 0.04$ [31]. [b] Ref. [32]. [c] $q_F = 0.27$ [33]. [d] Ref. [34].
[e] $q_F \approx 0.02$, own measurement. [f] $q_F = 0.60$ [33]. [g] $q_F = 0.62$ [33]. [h] Ref. [35].

the cyanine dye DTDC (IX) are listed in fig. 2. Characteristic absorption and emission data together with fluorescence lifetimes and experimen-

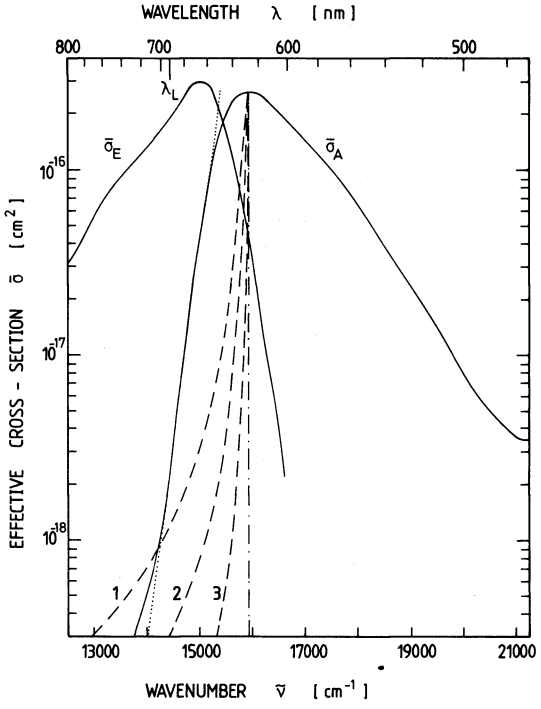

Fig. 3. Absorption and emission spectrum of nile blue sulfate dissolved in ethanol. Dotted line, fitted exponential rise of absorption $\bar{\sigma}_A \propto \exp(-|\nu - \nu_{A,m}|h/kT)$ with $T = 295$ K. Dashed curves: low-frequency part of homogeneous line shape centered at $\tilde{\nu}_{A,m} = \nu_{A,m}/c = 15924\ cm^{-1}$; (1) $\Delta\tilde{\nu}_H = 200\ cm^{-1}$, (2) $\Delta\tilde{\nu}_H = 100\ cm^{-1}$, (3) $\Delta\tilde{\nu}_H = 40\ cm^{-1}$.

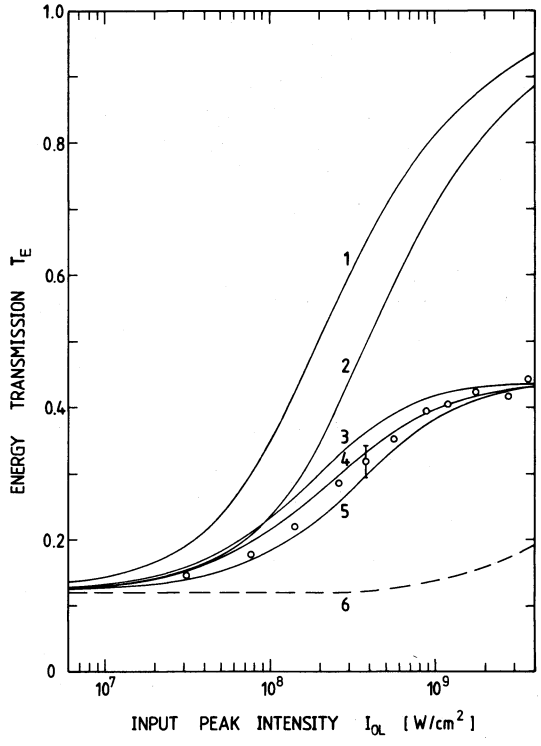

Fig. 4. Energy transmission versus input peak intensity. Dye nile blue sulfate dissolved in ethanol. Cell length 3 cm. Reorientation time $\tau_{or} = 220$ ps [34]. Pulse duration $\Delta t_L = 25$ ps (fwhm). Curves are calculated for (1) $\sigma_{ex} = 0$ and $T_3 = \infty$; (2) $\sigma_{ex} = 0$ and $T_3 \ll \Delta t_L$; (3) $\sigma_{ex} = 1.4\times10^{-16}\ cm^2$ and $T_3 = \infty$, (4) $\sigma_{ex} = 10^{-16}\ cm^2$ and $T_3 = \Delta t_L$, (5) $\sigma_{ex} = 7\times10^{-17}\ cm^2$ and $T_3 \ll \Delta t_L$. Dashed curve, $\rho_A = 1$, $\sigma_L = \bar{\sigma}_L = \alpha_L/N = 1.7\times10^{-18}\ cm^2$, $\sigma_{ex} = 7\times10^{-19}\ cm^2$; eqs. (2)–(6) are used with $N_1(\theta) = N_0(\theta)$. Other dye parameters are listed in table 1.

tally determined excited-state absorption cross sections are listed in table 1. As an example we give detailed curves for the dye nile blue sulfate dissolved in ethanol in the following.

The effective absorption spectrum $\bar{\sigma}_A(\lambda) = \alpha(\lambda)/N$ and the effective emission spectrum $\bar{\sigma}_E(\lambda)$ are displayed in fig. 3. The position of the laser wavelength λ_L is indicated.

The energy transmission T_E versus input peak intensity I_{0L} is plotted in fig. 4. Experimental points together with calculated curves are shown. Curves 1 and 2 are calculated for $T_3 = \infty$ and $T_3 \ll \Delta t_L$ [eq. (1) replaced by $N_1(\theta, t') = \rho_A N_0(\theta, t')$], respectively. The excited-state absorption cross section is set to $\sigma_{ex} = 0$. A factor of 2 higher pulse intensity is needed for $T_3 \ll \Delta t_L$ compared to $T_3 = \infty$ in order to bleach the dye to the same energy transmission. The refilling of level 1 within the pump pulse duration in case of $T_3 \ll \Delta t_L$ is responsible for the reduced bleaching. The excited-state absorption cross section σ_{ex} is obtained by fitting the theoretical curves to the experimental points. The σ_{ex} value depends on the cross-relaxation time T_3 since for $T_3 \gg \Delta t_L$ the number density $N_2(I_{0L} \to \infty) \approx \rho_A(\nu_L)N/2$ is approximating a factor of two smaller than for $T_3 \ll \Delta t_L$, where the population of level 2 approaches $N_2(I_{0L} \to \infty) \approx \rho_A(\nu_L)N/(1 + \rho_A)$ (see above). The curves 3 ($T_3 = \infty$, $\sigma_{ex} = 1.4 \times 10^{-16}$ cm^2), 4 ($T_3 = \Delta t_L = 25$ ps, $\sigma_{ex} = 10^{-16}$ cm^2) and 5 ($T_3 \ll \Delta t_L$, $\sigma_{ex} = 7 \times 10^{-17}$ cm^2) clearly demonstrate this fact. They fit to the experimental energy transmission at high input peak intensities.

The spectral cross-relaxation T_3 has to be longer than half the dephasing time T_2 ($T_3 \geqslant T_2/2$), since T_3 contributes to T_2 ($T_2^{-1} = (2T_3)^{-1} + (T_2')^{-1}$; T_2 phase relaxation time of level 1; T_2' pure dephasing time of level 1; T_3 energy relaxation time of level 1, here specially spectral cross-relaxation time). A lower limit of the dephasing time T_2 may be estimated from the spectral shape of the absorption spectrum in the long-wavelength tail. The shape of the absorption spectrum generally is determined by a convolution of transitions between rovibrational levels in the S_0 and S_1 band, by thermal level population, by inhomogeneous S_0–S_1 transition spacing due to irregular solute–solvent interaction, and by homogeneous broadening.

The spectral shape of the absorption spectrum in the long-wavelength wing is sometimes governed by thermal level population. The dotted line in fig. 3 indicates the expected rise of absorption due to thermal level population [$\bar{\sigma}_A(\nu) \propto \exp(-|\nu - \nu_{A,m}|h/kT)$] at $T = 295$ K. The slope of the absorption curve could not be fitted for all investigated substances to the experimental room temperature (e.g. fitted temperature is 250 K in case of oxazine 1 and 370 K in case of toluidine blue 0) indicating influences of inhomogeneous broadening and Franck–Condon factors. Out in the long-wavelength wing the absorption cross section decays more slowly than expected from thermal population (exponential decrease) or inhomogeneous origin (gaussian decrease). This fact is seen by the deviation of the $\bar{\sigma}_A$ curve from the dotted line in fig. 3. The reduced decrease of $\bar{\sigma}_A$ is most probably due to homogeneous broadening (lorentzian shape). Contributions of triplet absorption and dimer absorption cannot be completely excluded.

Three homogeneous line shapes of homogeneous linewidth $\Delta\tilde{\nu}_H = 200$ cm^{-1} (curve 1), $\Delta\tilde{\nu}_H = 100$ cm^{-1} (curve 2) and $\Delta\tilde{\nu}_H = 40$ cm^{-1} (curve 3) are included in fig. 3. The shape of curve 3 ($\Delta\tilde{\nu}_H = 40$ cm^{-1}) fits the shape of the absorption spectrum in the very-low-frequency wing. Since other mechanisms might contribute to the absorption spectrum in this region, $\Delta\tilde{\nu}_H = 40$ cm^{-1} gives only an upper limit of the homogeneous linewidth.

The homogeneous linewidth $\Delta\tilde{\nu}_H$ (fwhm) is related to the dephasing time by $T_2 = 1/\pi c \Delta\nu_H$ [22,30]. In the case of nile blue sulfate dissolved in ethanol we estimate $T_2 \gtrsim 2.5 \times 10^{-13}$ s ($T_3 > T_2/2$). Reported T_2 values of organic dye solutions at room temperature are in the same time region (1,1′-diethyl-4,4′-quinocyanine iodide in ethanol: $T_2 = 0.2$–0.6 ps [23]; cryptocyanine in methanol: $T_2 = 0.6$–1 ps [25] and 0.1–1 ps [26], DDI in glycerin: $T_2 \approx 0.4 \pm 0.2$ ps [27]).

The energy transmission data also exclude a complete homogeneous transition [28–30]. In this case all molecules would take part in the absorption even at $\nu_L < \nu_{F,m}$ [$\rho_A(\nu_L) = 1$] and the nonlinear transmission should follow the dashed curve in fig. 4. The Rayleigh-induced optical Kerr-effect polarization results of ref. [28] might result from

spectral diffusion of excited molecules which extends the induced dichroism and birefringence over the whole inhomogeneously broadened band [29].

5. Conclusions

The dynamics of some dyes excited to the long-wavelength region of the S_0–S_1 absorption band has been investigated. The S_0–S_1 excitation is believed to terminate in the potential minimum of the S_1 state (Franck–Condon state and temporal equilibrium state coincide). As a consequence no inversion is achievable for the region of optimum stimulated emission cross section ($\nu > \nu_L$). Amplified spontaneous emission and net gain in a laser resonator are limited to the long-wavelength tail of the fluorescence band (reduced efficiency due to decreasing σ_E for $\nu < \nu_L$). Bleaching of dyes is readily observed and the application of saturable absorbers may be extended to the long-wavelength region of the S_0–S_1 transition [37,38].

Acknowledgement

The authors thank Th. Ascherl for technical assistance and the Rechenzentrum of the University for disposal of computer time.

References

[1] C.V. Shank, E.P. Ippen and O. Teschke, Chem. Phys. Letters 45 (1977) 291.
[2] W. Falkenstein, A. Penzkofer and W. Kaiser, Opt. Commun. 27 (1978) 151.
[3] A.H. Zewail, in: Springer Series in Chemical Physics, Vol. 23. Picosecond phenomena, Part III, eds. K.B. Eisenthal, R.M. Hochstrasser, W. Kaiser and A. Laubereau (Springer, Berlin, 1982) p. 184.
[4] C.S. Parmenter and K.Y. Tang, Chem. Phys. 27 (1978) 127.
[5] V. Sundström, T. Gillbro and H. Bergström, Chem. Phys. 73 (1982) 439.
[6] H. Staerk, R. Mitzkus, W. Kühnle and A. Weller, in: Springer Series in Chemical Physics, Vol. 23 Picosecond phenomena, Part III, eds. K.B. Eisenthal, R.M. Hochstrasser, W. Kaiser and A. Laubereau (Springer, Berlin, 1982) p. 205.
[7] M.E. Mack, Appl. Phys. Letters 15 (1969) 166.
[8] A. Penzkofer and W. Falkenstein, Opt. Quantum Electron. 10 (1978) 399.
[9] A. Müller, J. Schulz-Henning and H. Tashiro, Appl. Phys. 12 (1977) 333.
[10] J. Wiedmann and A. Penzkofer, Nuovo Cimento 63B (1981) 459.
[11] S.L. Chin and A. Zardecki, Phys. Rev. A13 (1976) 1528.
[12] S.L. Chin and D. Belanger, Opt. Commun. 16 (1976) 121.
[13] D. Faubert, S.L. Chin, M. Cormier and M. Boloten, Can. J. Phys. 57 (1979) 160.
[14] D. Faubert and S.L. Chin, Can. J. Phys. 57 (1979) 1359.
[15] D. Faubert and S.L. Chin, Can. J. Phys. 60 (1982) 261.
[16] D. Leupold, R. König, B. Voigt and R. Menzel, Opt. Commun. 11 (1974) 78.
[17] A. Penzkofer and W. Blau, Opt. Quantum Electron. 15 (1983) 325.
[18] O.G. Peterson, J.P. Webb, W.C. McColgin and J.H. Eberly, J. Appl. Phys. 42 (1971) 1917.
[19] A. Yariv, Quantum electronics, 2nd Ed. (Wiley, New York, 1975) ch. 15.
[20] W. Blau, R. Reber and A. Penzkofer, Opt. Commun. 43 (1982) 210.
[21] S.J. Strickler and R.A. Berg, J. Chem. Phys. 37 (1962) 814.
[22] M.D. Levenson, Introduction to nonlinear laser spectroscopy (Academic Press, New York, 1982).
[23] T. Yajima, H. Souma and Y. Ishida, Phys. Rev. A17 (1978) 324.
[24] H. Souma, T. Yajima and Y. Taira, J. Phys. Soc. Japan 48 (1980) 2040.
[25] G. Mourou, IEEE J. Quantum Electron. QE-11 (1975) 1.
[26] L. Huff and L.G. DeShazer, J. Opt. Soc. Am. 60 (1970) 157.
[27] D.W. Vahey and A. Yariv, Phys. Rev. A10 (1974) 1578.
[28] J.J. Song, J.H. Lee and M.D. Levenson, Phys. Rev. A17 (1978) 1439.
[29] Y. Taira and T. Yajima, J. Phys. Soc. Japan 50 (1981) 3459.
[30] A. Penzkofer, A. Laubereau and W. Kaiser, Progr. Quantum Electron. 6 (1979) 55.
[31] J. Olmsted III, J. Phys. Chem. 83 (1979) 2581.
[32] G.S. Beddard, T. Doust and G. Porter, Chem. Phys. 61 (1981) 17.
[33] R. Sens and K.H. Drexhage, J. Luminescence 24/25 (1981) 709.
[34] H.E. Lessing and A. von Jena, in: Laser handbook, Vol. 3, ed. M.L. Stitch (North-Holland, Amsterdam, 1979) p. 784.
[35] W. Sibbett, J.R. Taylor and D. Welford, IEEE J. Quantum Electron. QE-17 (1981) 500.
[36] M.W. McGeoch, Opt. Commun. 7 (1973) 116.
[37] E.G. Arthurs, D.J. Bradley, P.N. Puntambekar, I.S. Ruddock and T.J. Glynn, Opt. Commun. 12 (1974) 360.